

Colorimetric Detection of Mercury(II) Ion Using Unmodified Silver Nanoparticles and Mercury-Specific Oligonucleotides

Yong Wang,^{†,‡} Fan Yang,[†] and Xiurong Yang^{*,†}

State Key Laboratory of Electroanalytical Chemistry, Changchun Institute of Applied Chemistry, Chinese Academy of Sciences, Changchun, Jilin 130022, China, Graduate School of the Chinese Academy of Sciences, Beijing 100039, China

ABSTRACT A sensitive and selective colorimetric detection method for mercury(II) has been well-established in this paper. It was based on the conformation change of mercury-specific oligonucleotides (MSO) from random coil structure to hairpin structure upon the addition of Hg²⁺ and the phenomenon of salt-induced unmodified silver nanoparticles (AgNPs) aggregation. The calibration curve showed that the net absorption ratio value at 395 and 570 nm increased linearly over the Hg²⁺ concentration range of 25–500 nM with a limit of detection of 17 nM. The other environmentally relevant metal ions did not interfere with the determination of Hg²⁺.

KEYWORDS: mercury(II) ion • mercury-specific oligonucleotides • unmodified silver nanoparticles • thymine–Hg²⁺–thymine coordination • colorimetry

Up to now, optical biosensors, especially those colorimetric biosensors (1), have been fast becoming the methods of choice in a lot of biosensing application. Although many reports have described the application of chromophoric colorimetry, most of them displayed limitations in practical use, such as poor sensitivity, and in certain cases the applications are not stable or not functional in aqueous environments (2, 3).

To resolve these issues, noble metallic nanoparticles, in particular gold nanoparticles (AuNPs), have recently emerged as important colorimetric reporters because their extremely high visible-region extinction coefficients (1×10^8 to $1 \times 10^{10} \text{ M}^{-1} \text{ cm}^{-1}$) are often several orders of magnitude higher than those of organic dyes and their surface plasmon resonance (SPR) absorption is strongly distance-dependent (4). However, unfunctionalized AuNPs show poor selectivity in responding to analytes. Thus, the functionalization of AuNPs with DNA molecules (aptamer, DNAzyme and their combination) provide a possibility for selective colorimetric biosensing and have recently been used to detect a broad range of analytes (5–7). However, the modification of functional DNA onto the AuNPs and the separation of the modified AuNPs from the unmodified AuNPs or surplus aptamers were often required. Obviously, these steps were rather time-consuming and relative highly costly. Thus, the development of modification-free AuNPs colorimetric bio-

sensors to simplify the detection process would be important and attractive.

Until recently, Rothberg's group reported a novel DNA biosensor using unmodified AuNPs colorimetric sensing based on the discriminated stable effects of different DNA structures adsorbed onto the nanoparticles (8). Subsequently, many researchers extended this target of the unmodified methods to various analytes, such as small molecules (9, 10), metal ions (11, 12), and protein (13). Almost all the research focus on this issue has been concerned with using AuNPs with little work on other noble metallic nanoparticles such as silver nanoparticles (AgNPs) (14–17). This may be due to the chemical degradation of the AgNPs under the functionalization conditions and the susceptibility of silver surface to oxidation (14). However, the benefit of using AgNPs rather than AuNPs is that the molar extinction coefficient is 100-fold greater, therefore increasing sensitivity when using absorption spectroscopy, which leads to improved visibility due to the difference in optical brightness (18).

In this letter, a sensitive and selective colorimetric biosensor for environmentally toxic mercury(II) ion (Hg²⁺) was constructed by coupling the unique optical properties of water-soluble unmodified AgNPs with Hg²⁺-binding specificity of a functional DNA probe (mercury-specific oligonucleotide). The principle based on AgNPs colorimetric biosensing is similar to that of AuNPs. Very recently, it has been reported that unfolded single-stranded DNA (ssDNA) showed high binding ability toward unmodified AgNPs, but double-stranded DNA (dsDNA) did not (15–17). This suggests that similar to AuNPs, unmodified AgNPs can also possibly be employed to probe DNA target-responsive structural variation, such as the change from unfolded ssDNA conformation to rigid dsDNA or hairpin structure. On the other hand, it

* Corresponding author. Tel.: +86 431 85262056. Fax: +86 431 85689278. E-mail: xryang@ciac.jl.cn.

Received for review October 22, 2009 and accepted February 1, 2010

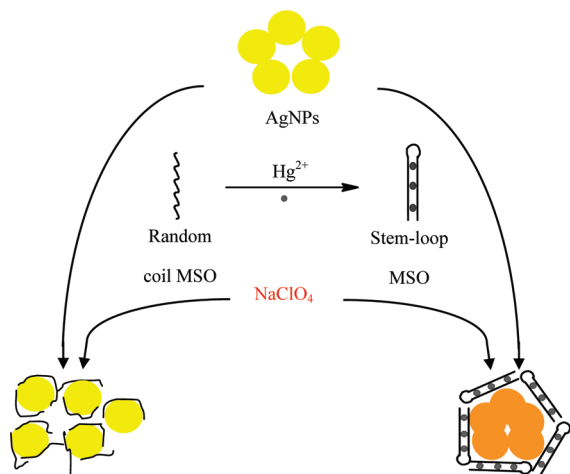
[†] Changchun Institute of Applied Chemistry, Chinese Academy of Sciences.

[‡] Graduate School of the Chinese Academy of Sciences.

DOI: 10.1021/am9007243

© 2010 American Chemical Society

Scheme 1. Strategy for Colorimetric Biosensing of Hg^{2+} Based on AgNPs and MSO



has been previously demonstrated that Hg^{2+} can selectively bind in between two DNA thymine bases to form stable T– Hg^{2+} –T base pairs (19, 20). This Hg^{2+} -mediated T–T base pair is able to direct the folding of single-stranded DNA into hairpin or duplexes, thus many colorimetric biosensors for Hg^{2+} ions can be developed using thymine (T)-containing oligonucleotides of elaborate design as recognition elements and unmodified AuNPs as reporting probes (21–25). In this work, T-containing oligonucleotides proposed by Willner's group (25) are selected for mercury-specific oligonucleotides (MSO). It was reported that the presence of Hg^{2+} enabled the unfolded T-containing oligonucleotides to fold into a rigid stem-loop (hairpin) structure in which the T residues of the spatially separated nucleotides were linked by the Hg^{2+} ions, and the stiff hairpin structure of the Hg^{2+} -bridged DNA, similarly to duplex DNA, could not wrap around and stabilize AuNPs, leading to their aggregation under the high-salt conditions (25). Therefore, under conditions similar to those employed by Willner's group, a colorimetric biosensor for Hg^{2+} can be possibly constructed using AgNPs instead of AuNPs as reporting probes.

Scheme 1 shows the AgNPs-MSO colorimetric strategy for Hg^{2+} detection. As displayed in Scheme 1, unmodified AgNPs are stable because of the negative capping agent's (i.e., citrate) electrostatic repulsion against van der Waals attraction between AgNPs. Thus, the addition of enough salt (NaClO_4) screens the repulsion between unmodified AgNPs and gives rise to the aggregation of the AgNPs which provokes a corresponding yellow-to-red color change. It was previously reported that amines could bind exceptionally strongly with AgNPs, which was similar to AuNPs (26, 27). Therefore, it is reasonable for us to believe that there is stronger coordination interaction between the nitrogen atoms of the random coil ssDNA and AgNPs than electrostatic repulsion between the negative-charged phosphate backbone and the negative-charged AgNPs. This suggests that the random coil MSO (ssDNA) also adsorbs onto the AgNPs and facilitates to enhance the AgNPs' stability against salt-induced aggregation (solution remains yellow). Upon the addition of Hg^{2+} , the folding of random coil MSO can be

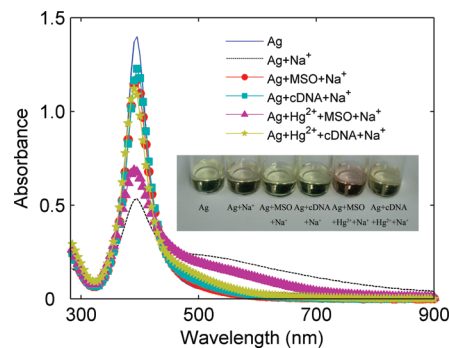


FIGURE 1. UV-visible absorption spectra and photographs (inset) of 0.075 nM AgNPs under different experimental conditions. Other experimental conditions are $c_{\text{Hg}^{2+}} = 500$ nM, $c_{\text{Na}^+} = 50$ mM, $c_{\text{MSO}} = c_{\text{cDNA}} = 500$ nM.

directed by stable T– Hg^{2+} –T base pairs into a rigid stem-loop structure. The rigid structure prevents the exposure of the MSO bases to the AgNPs and the high density of negative charges increases the repulsion between the MSO and the AuNPs. As a result, the rigid structure can not adsorb onto the AgNPs and loses the ability to protect AgNPs, leading to a color change from yellow to red.

When the proof-of-concept experiments were performed, it could be clearly observed from Figure 1 that the citrate-stabilized AgNPs showed an intense surface plasmon resonance (SPR) absorption band peaked at 395 nm, and thus exhibited a vivid yellow color. Following the addition of the salt (NaClO_4) to the AgNPs, the SPR band broadened and red-shifted significantly from 395 to 570 nm. This broadening and red shifting was a result of salt-induced AgNPs aggregation, which could be observed with the naked eye in the form of a color change from vivid yellow to pale red. However, in the presence of ssDNA (unfolded MSO and cDNA), the SPR band of AgNPs after adding salt remained almost unchanged, displaying the intrinsic absorption peak at 395 nm, and the corresponding yellow color remained. This indicated that ssDNA adsorbed onto the AgNPs and helped to enhance the AgNPs' stability against salt-induced aggregation. Following the addition of Hg^{2+} to MSO–AgNP–salt solution, it was observed that the intensity of 395 nm peak decreased and shifted to longer wavelength, while the intensity of the absorption band at 570 nm increased. Correspondingly, the color of the AgNPs solution changed from yellow to pale red. A direct evidence for Hg^{2+} -stimulated aggregation of the AgNPs could be further supported by transmission electron microscopy (TEM) measurements that revealed individual nanoparticle (NP) in the absence of Hg^{2+} (Figure 2A) and aggregation of NPs in the presence of Hg^{2+} (Figure 2B). Therefore, it was supposed that binding of Hg^{2+} with unfolded MSO forms a hairpin-structured MSO; this relatively rigid structure reduces the exposure of the DNA bases to AgNPs, and loses the ability to disperse the AgNPs. To further support the reasoning, we conducted control experiments using cDNA under similar conditions. As expected, the addition of Hg^{2+} did not induce any noticeable change in their UV-visible spectrum of AgNPs solution, and the yellow color remained unchanged. This suggested that MSO were selective Hg^{2+} recognition elements in the system.

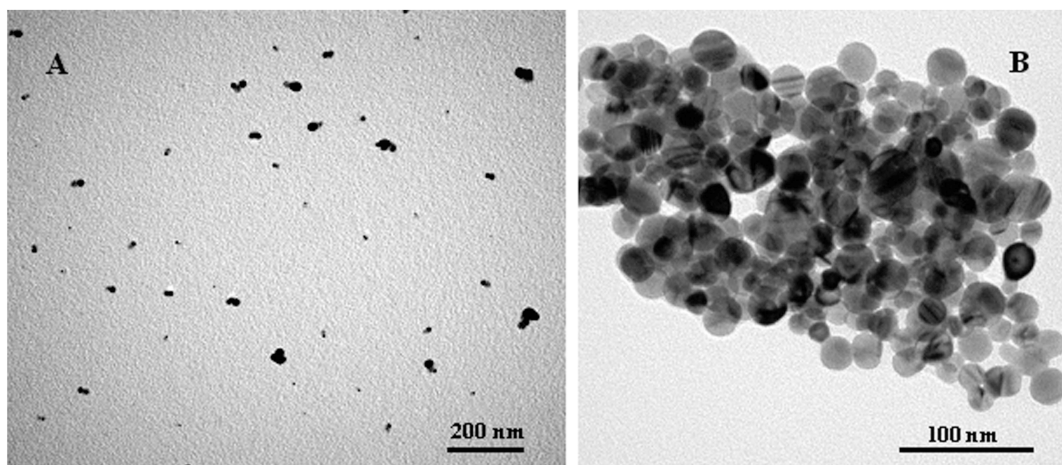


FIGURE 2. TEM images of the AgNPs solution (0.075 nM) mixed with 300 nM MSO in the (A) absence or (B) presence of 500 nM Hg^{2+} after the addition of 60 mM NaCl.

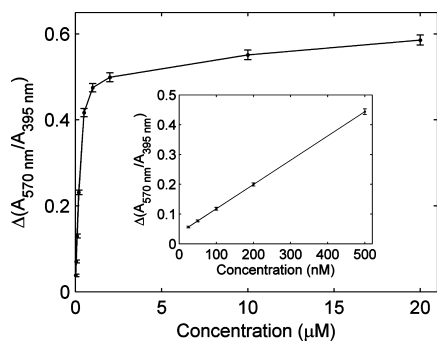


FIGURE 3. Net absorption ratio ($A_{570 \text{ nm}}/A_{395 \text{ nm}}$) of AgNPs vs Hg^{2+} concentration. Other experimental conditions are $c_{\text{Na}^+} = 60 \text{ mM}$, $c_{\text{MSO}} = 100 \text{ nM}$. The error bars represent the standard deviation of three measurements.

The sensitivity of AgNPs probe toward Hg^{2+} was investigated. Several calibration samples with different concentrations of Hg^{2+} (three measurements for each concentration) were analyzed, and UV–visible absorption spectra were collected. The net absorption ratio value, $\Delta(A_{570 \text{ nm}}/A_{395 \text{ nm}})$, as a function of the concentration of Hg^{2+} (0.025 μM to 20 μM) was plotted in Figure 3. As could be seen, the net absorption ratio value rapidly increased up to 500 nM with the increase in the concentration of Hg^{2+} . A linear correlation ($r = 0.9997$) existed between the net absorption ratio value and the concentration of Hg^{2+} over the range of 25–500 nM. The limit of detection (LOD) was calculated to be 17 nM ($S/N = 3$), which could be comparable or superior to those of the assays based on AuNPs or fluorescent dyes (21–25, 28).

The selectivity of this assay approach toward Hg^{2+} was evaluated by testing the net absorption ratio value to other environmentally relevant metal ions, including Mg^{2+} , Ca^{2+} , Fe^{2+} , Fe^{3+} , Cd^{2+} , Co^{2+} , Cu^{2+} , Mn^{2+} , Ni^{2+} , Pb^{2+} and Zn^{2+} at a concentration of 500 nM. As can be observed in Figure 4, only the Hg^{2+} showed a significantly larger net absorption ratio value as compared to other metal ions, indicating that the assay approach has very high specificity toward Hg^{2+} .

In conclusion, a simple and cost-effective assay using MSO and AgNPs for the sensitive and selective detection of Hg^{2+} ions was developed. Although we have used this system to demonstrate the detection of Hg^{2+} ions only, this

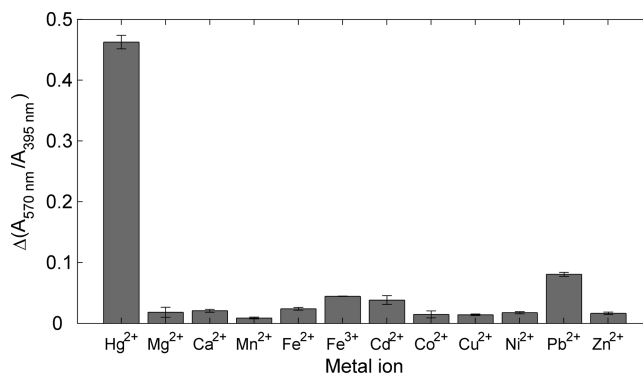


FIGURE 4. Net absorption ratio ($A_{570 \text{ nm}}/A_{395 \text{ nm}}$) of AgNPs in the presence of different metal ions. The concentration of all metal ions was 500 nM. Other experimental conditions are as in Figure 2. The error bars represent the standard deviation of three measurements.

AgNPs-based colorimetric method could be further applied to the determination of other metal ions, small molecules, or proteins by using other specific DNA-based sensing elements. Further work toward this direction is underway.

Acknowledgment. This work was supported by the National Natural Science Foundation of China (20890022), the National Key Basic Research Development Project of China (2010CB933602), and the Project of Chinese Academy of Sciences (KJ CX2-YW-H09).

Supporting Information Available: Experimental details regarding preparation of citrate-stabilized silver nanoparticles and general procedure of colorimetric detection of Hg^{2+} (PDF). This material is available free of charge via the Internet at <http://pubs.acs.org>.

REFERENCES AND NOTES

- Hall, D. *Anal. Biochem.* **2001**, *288*, 109–125.
- Wan, Y. J.; Niu, W. J.; Behof, W. J.; Wang, Y. F.; Boyle, P.; Gorman, C. B. *Tetrahedron* **2009**, *65*, 4293–4297.
- Cheng, Y. F.; Zhang, M.; Yang, H.; Li, F. Y.; Yi, T.; Huang, C. H. *Dyes Pigm.* **2008**, *76*, 775–785.
- Yguerabide, J.; Yguerabide, E. E. *Anal. Biochem.* **1998**, *262*, 137–156.
- Chen, S. J.; Huang, Y. F.; Huang, C. C.; Lee, K. H.; Lin, Z. H.; Chang, H. T. *Biosens. Bioelectron.* **2008**, *23*, 1749–1753.
- Huang, C. C.; Huang, Y. F.; Cao, Z. H.; Tan, W. H.; Chang, H. T. *Anal. Chem.* **2005**, *77*, 5735–5741.

- (7) Lu, Y.; Liu, J. W. *Acc. Chem. Res.* **2007**, *40*, 315–323.
- (8) Li, H. X.; Rothberg, L. *Proc. Natl. Acad. Sci. U.S.A.* **2004**, *101*, 14036–14039.
- (9) Wang, J.; Wang, L. H.; Liu, X. F.; Liang, Z. Q.; Song, S. P.; Li, W. X.; Li, G. X.; Fan, C. H. A. *Adv. Mater.* **2007**, *19*, 3943–3946.
- (10) Zhang, J.; Wang, L. H.; Pan, D.; Song, S. P.; Boey, F. Y. C.; Zhang, H.; Fan, C. H. *Small* **2008**, *4*, 1196–1200.
- (11) Li, B. L.; Du, Y.; Dong, S. J. *Anal. Chim. Acta* **2009**, *644*, 78–82.
- (12) Wei, H.; Li, B. L.; Li, J.; Dong, S. J.; Wang, E. K. *Nanotechnology* **2008**; 095501.
- (13) Wei, H.; Li, B. L.; Li, J.; Wang, E. K.; Dong, S. J. *Chem. Commun.* **2007**, 3735–3737.
- (14) Wei, H.; Chen, C. G.; Han, B. Y.; Wang, E. K. *Anal. Chem.* **2008**, *80*, 7051–7055.
- (15) Su, X. D.; Kanjanawarut, R. *ACS Nano* **2009**, *3*, 2751–2759.
- (16) Kanjanawarut, R.; Su, X. D. *Anal. Chem.* **2009**, *81*, 6122–6129.
- (17) Xu, X. W.; Wang, J.; Yang, F.; Jiao, K.; Yang, X. R. *Small* **2009**, *5*, 2669–2672.
- (18) Thompson, D. G.; Stokes, R. J.; Martin, R. W.; Lundahl, R. J.; Faulds, K.; Graham, D. S. *Small* **2008**, *4*, 1054–1057.
- (19) Miyake, Y.; Togashi, H.; Tashiro, M.; Yamaguchi, H.; Oda, S.; Kudo, M.; Tanaka, Y.; Kondo, Y.; Sawa, R.; Fujimoto, T.; Machinami, T.; Ono, A. *J. Am. Chem. Soc.* **2006**, *128*, 2172–2173.
- (20) Tanaka, Y.; Oda, S.; Yamaguchi, H.; Kondo, Y.; Kojima, C.; Ono, A. *J. Am. Chem. Soc.* **2007**, *129*, 244–245.
- (21) Liu, C. W.; Hsieh, Y. T.; Huang, C. C.; Lin, Z. H.; Chang, H. T. *Chem. Commun.* **2008**, 2242–2244.
- (22) Xu, X. W.; Wang, J.; Jiao, K.; Yang, X. R. *Biosens. Bioelectron.* **2009**, *24*, 3153–3158.
- (23) Yu, C. J.; Cheng, T. L.; Tseng, W. L. *Biosens. Bioelectron.* **2009**, *25*, 204–210.
- (24) Li, L.; Li, B. X.; Qi, Y. Y.; Jin, Y. *Anal. Bioanal. Chem.* **2009**, 393, 2051–2057.
- (25) Li, D.; Wieckowska, A.; Willner, I. *Angew. Chem., Int. Ed.* **2008**, *47*, 3927–3931.
- (26) Basu, S.; Jana, S.; Pande, S.; Pal, T. J. *Colloid Interface Sci.* **2008**, *321*, 288–293.
- (27) Nath, S.; Ghosh, S. K.; Kundu, S.; Praharaaj, S.; Panigrahi, S.; Pal, T. J. *Nanopart. Res.* **2006**, *8*, 111–116.
- (28) Vaswani, K. G.; Keranen, M. D. *Inorg. Chem.* **2009**, *48*, 5797–5800.

AM9007243